

Observation of Vessel Heave with Airborne SAR

M.D. Henschel^a and C.E. Livingstone^b

^aMacDonald, Dettwiler, and Associates (under contract to DRDC Ottawa),
email: michael.henschel@drdc-rddc.gc.ca;

^bDefence R&D Canada – Ottawa, email: chuck.livingstone@drdc-rddc.gc.ca

ABSTRACT

Ships moving on the ocean surface experience forcing from both the propulsion system and the dynamics of the ocean surface. To fully categorize the vessel motion, it is necessary to estimate the motion of a ship in both the horizontal plane (track made good) and the vertical (heave) direction. Over the period of illumination with an airborne (and perhaps spaceborne) SAR, both horizontal and vertical motions of a ship can be observed. Reliable estimates of vessel velocity require that heave motion be accounted for over the radar observation period to compensate for the most significant acceleration terms during image formation.

This paper presents a methodology for the extraction of heave motion from vessels at sea and describes the contribution of this motion to radar measurements of ship velocity. The extracted, time varying heave motion is shown to be a necessary contributor to matched filter algorithms used to focus SAR images of moving vessels. Heave is, thus, shown to be needed for robust estimates of vessel velocity components parallel to the SAR direction of travel. To demonstrate the impact of ship heave on SAR GMTI performance, a heave extraction and compensation methodology is described and applied to vessels from two different experiment trials conducted using the C-Band Along-Track Interferometric SAR on board the Environment Canada CV-580 aircraft with different vessels and sea states. The results show that the vessel velocity is well modelled at least for larger ships and low to moderate sea states.

Keywords: Ground Moving Target Indication, SAR Processing, Ship Detection, Ship Motion

1 INTRODUCTION

Modelling the motion of targets on the ocean surface differs distinctly from the terrestrial case. With a ship we can assume a narrow range of horizontal (along and across track) motions but we must also assume that a dynamic vertical component of motion due to the ocean surface is present. This paper will present a physical parametrization of vessel motion that accounts for the heave motion of the vessel. The heave motion of the vessel is derived from a time-frequency decomposition and then used to define a matched filter that enables the calculation of along and across track velocities. The parametrization also provides better focussing of the SAR imagery. Achieving a verifiable model for the observation of ship dynamics is of interest in applications for search and rescue, where the dynamics of a vessel may indicate the safety of the people on board, and in ocean monitoring, where the motion of a vessel makes ship detection more complicated.

SAR systems are exceptionally good tools to determine target motion ([1], for instance). There has been a good deal of excellent work accomplished in the use of time-frequency methods ([2], [3], and [4]) and matched filter bank methods ([5] and [6]) to explain the effects of velocity and acceleration in the imaging of moving targets. These methods have either considered the terrestrial case where an object has been assumed to be moving without a vertical velocity component or they have assumed that the motion of a target can be modelled with a polynomial approximation ([7]). While the latter is correct, the derivation presented here provides a more physical description of the phenomena of radar imaging of a moving ship.

In the case of a large vessel in transit on the ocean surface, we can assume that the motion in the horizontal plane is due primarily to the propulsion forces (propellers, winds, and currents) and that the main accelerations are due to course changes. Motion in the vertical direction will be due to the encounter of waves on the ocean surface as filtered by the vessel inertia. Dynamic stabilization of larger vessels is normally used to reduce the components

of roll and yaw motion such that it may be safe to ignore these components. Consequently propulsion and vertical motion acting over the length of the vessel should account for most of the movement of a larger vessel imaged by a radar.

A parametrization of a model for ship motion observed by SAR is presented in Section 2. The application of the model to data is discussed in Section 3 with ground truth data discussed in Section 4. The experiments used to validate the model were performed using the C-Band Along-Track Interferometric (ATI) SAR on the Environment Canada Convair-580 research aircraft [8]. Data taken, of the M/V Green Guatemala (see Figure 1), a 131m long refrigeration ship, on 12 June 2006 offshore Newfoundland, Canada are used to illustrate the discussion in the following sections.



Figure 1. The M/V Green Guatemala. (Image courtesy of Green Chartering AS.)

2 BACKSCATTER FROM A MOVING SHIP

The return signal from a point target may be modelled as

$$s(t) = A(t) \exp(-ik2R(t)), \quad (1)$$

where $A(t)$ is the time varying magnitude of the returns; the phase depends on the radar wavenumber, k , and the (two-way) path distance to the target is $2R(t)$.

An important characteristic of the signal backscattered from a vessel at sea is the time duration of the usable returns. The magnitude of the returns from a ship are much larger than the returns from the ocean surface. The duration of the signal, for which $A(t)$ is large, is typically longer than the -3dB beamwidth of the radar. The ATI SAR imagery used in this analysis provided a signal duration equal to approximately a -12 dB beamwidth – even at this beamwidth, the returns examined are from the main lobe. The side lobe suppression in the radar system used is strong ([8]). The length of the return signal impacts on two aspects of the analysis: 1) range walk compensation, and 2) the ability to extract the target history. A shorter time series makes the calculation of frequency components from the target history increasingly difficult. These components can still be used to aid in the focussing of the target signature (see for instance [9]), but the geophysical parameters to which they are attributed would be masked by the short duration. In this sense, the concepts developed here can be applied more easily to an airborne SAR – where the target illumination time is long enough. Any steerable SAR system, whether airborne or spaceborne, would exhibit an increased target dwell time and hence we can expect to be able to more fully exploit the signature of a vessel with such systems.

Range walk compensation is clearly important in a system that exploits a -12 dB beamwidth. A number of algorithms are available for range walk compensation. The relative strength of the ship return compared to the ocean, makes the isolation of the ship target returns relatively easy in the range compressed data. By considering the shape of the target returns in the range compressed data, it is possible to perform range walk correction using a sinc function (as described in [10]). The extent of the range walk has been estimated by fitting a quadratic expression to the peak returns. The radar range resolution (on the order of 4 m) is large enough in the airborne case that we do not need to consider higher order contributions to the range curvature. Other methods of identifying the range walk (without reference to external data sources) have been published recently with particular application to identifying the Doppler ambiguity (e.g., [11] and [12]).

Figure 2 shows the azimuth uncompressed returns following range walk compensation for the M/V Green Guatemala. It is clear that at least two main scattering centres are responsible for the returns from the ship. The M/V Green Guatemala (see Figure 1) has cranes and lattice like structures that explain the existence of areas of relatively high return power.

By considering the imaging geometry described by Figure 3, we can derive an expression for the distance between the ship and the radar sensor. The beam centre on the ground is assumed to be travelling with a constant velocity, v_a , in the positive x direction. The ship is modelled with linear accelerations in the x and y directions

and a sinusoidally varying motion in the direction of the z axis. The time varying distance between the radar and the ship target can be expressed as

$$R(t) = \sqrt{\left((v_a - v_x)t + \frac{a_x}{2}t^2\right)^2 + \left(y_0 + v_y t + \frac{a_y}{2}t^2\right)^2 + \left(z_0 + \sum \vec{a} \cos(\vec{\omega}t + \vec{\psi})\right)^2}, \quad (2)$$

where the position of the ship at $t=0$ is $(0, y_0, z_0)$, the constant along and across track velocities are v_x , and v_y , respectively, the accelerations of the ship in x and y are given as a_x and a_y , and, finally, the sinusoidal variations in height are given as the sum of the components of a wave with amplitudes, \vec{a} , frequencies of encounter, $\vec{\omega}$, and phases of encounter, $\vec{\psi}$.

From this formulation, the Maclaurin series can be derived to show the relative importance of each term. By neglecting terms on the order of $R(t)^{-3}$ and smaller, the series can be written:

$$R(t) \approx R_0 + \frac{y_0 v_y + (z_0 + \zeta_0) \zeta_0'}{R_0} t + \frac{2(v_a - v_x)^2 + 2v_y^2 + 2a_y y_0 + z_0 \zeta_0'' + (\zeta_0')^2 \zeta_0 \zeta_0''}{4R_0} t^2, \quad (3)$$

where, for convenience, ζ is substituted for the expression $\sum \vec{a} \cos(\vec{\omega}t + \vec{\psi})$ in (2) and R_0 is the range distance evaluated at $t = 0$. The relative contributions to the range distance from across track and vertical velocities and accelerations are very large compared to the along track velocity. It is clear from (3) that the strength of the variations in the z direction are strong enough to have a discernible effect on the range to target. The effects of velocity and acceleration on the matched filter processing of a point target moving along the ground has been described in [5].

Standard range-Doppler algorithms (see, for instance [10]) assume a matched filter processing based on a stationary target. In this case the matched filter is based on the phase return of a signal with the target motion in (2) set to zero.

Comparing the convolution of the signal, $s(t)$, with a matched filter $g(t) = \exp(ik2R(t))$, illustrates the problem. Inclusion of across track velocity in the signal, but not the matched filter, causes the matched filter result to be azimuth shifted ([1]). If across and along track velocities are included in the signal then the result is both smeared and shifted in azimuth (as shown by the green line in Figure 4). Adding heave to the signal results in further complication. This is shown as the red line, in Figure 4, where the effects of quickly varying accelerations deform from the response shown by the green line. In each case, the magnitude of the target response is diminished from the stationary case with the addition of motion characteristics – which provides the motivation to consider a more detailed analysis of the backscattered signal, as described in the following.

The Doppler frequency of the signal backscattered from a target contains information about its motion. Doppler frequency is given as $f_D(t) = \frac{-1}{2\pi} \frac{\delta\phi}{\delta t}$, where ϕ is the phase given in (1). Taking $R(t)$ from (2) results in the expression:

$$f_D(t) \approx -\frac{k}{\pi R(t)} \left[\left((v_a - v_x)^2 + v_y^2 + y_0 a_y \right) t + y_0 v_y - z_0 \sum \vec{\omega} \vec{a} \sin(\vec{\omega}t + \vec{\psi}) \right]. \quad (4)$$

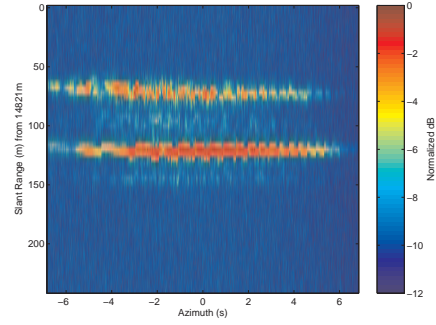


Figure 2. Range compressed, azimuth uncompressed returns from the M/V Green Guatemala after range walk compensation. The response shows two strong scattering centres separated by approximately 50 m (and corresponding to bright reflectors on the superstructure).

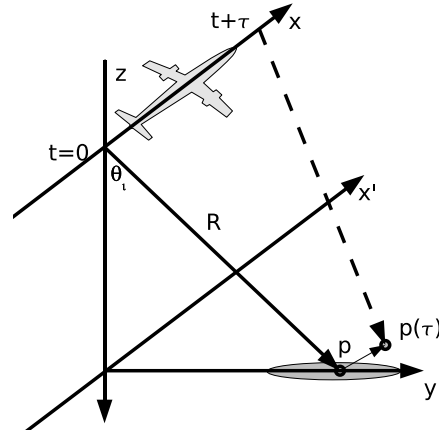


Figure 3. The geometry assumed for the imaging of a moving ship located at the point p when the aircraft is at time $t=0$.

Because the Doppler frequency is defined in terms of the phase of the return signal, it is more sensitive (than say the range walk) to small variations in target motion. From (4), it is clear that the constant horizontal velocities are represented by a straight line, in the plot of frequency as a function of time, and that the vertical motions can be considered as a superimposed periodic function. The across track acceleration also figures prominently in the Doppler rate obtained by taking the derivative with respect to time.

3 EXTRACTING SHIP MOTION CHARACTERISTICS

Using a high resolution technique, such as the Wigner-Ville time-frequency decomposition, we are able to extract the Doppler history of the backscattered signal (see, for example, [2], [4], or [13]). Other methods for identifying the instantaneous frequency are also available ([3] and [7]), however, the Wigner-Ville decomposition works well for this application. The linear component of the Doppler history is removed using a robust linear least squares fit to a straight line and the remaining (periodic) signature can be extracted using a high resolution spectral estimator. The fast orthogonal search (FOS) algorithm described by [14] and [15] works well for this purpose. The fitted line may be used to estimate v_x and v_y ; however, this method is not as sensitive to changes in v_x as we may desire: clearly a small across track acceleration will affect these estimates.

Following from our assumptions, the fitted periodic part of the Doppler history provides the encounter frequency and phase for the wave field as well as a measure of the Doppler frequency shift due to heave amplitude at a particular scattering centre. Phase variations of the $\zeta(t)$ function estimated from the backscatter of a cross track travelling vessel confirm wave field coupling to the vessel motion. Estimating the heave component, as $\hat{\zeta}(t)$, from the time-frequency decomposition is an efficient means of quantifying the nonlinear accelerations in the target response. These motions can then be accounted for in matched filter processing of the target signal.

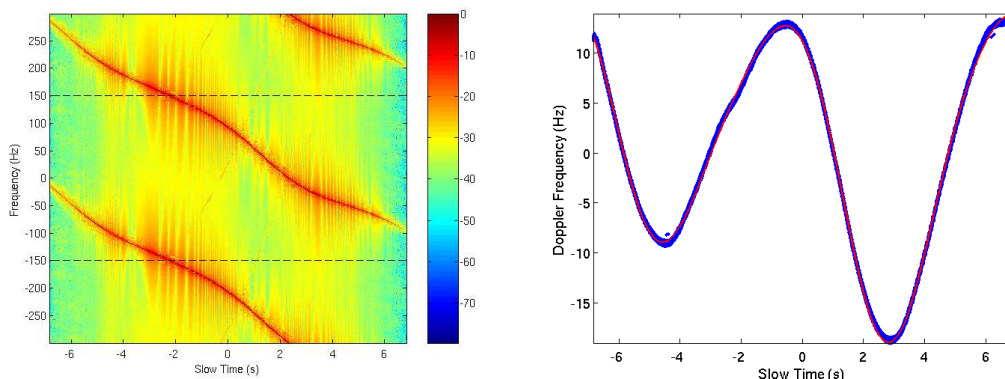


Figure 5. Wigner-Ville time-frequency decomposition of the return signal from the M/V Green Guatemala taken on 12 June 2006 (left). The graph on the right shows the heave signature found by isolating the linear components of the observed Doppler frequency.

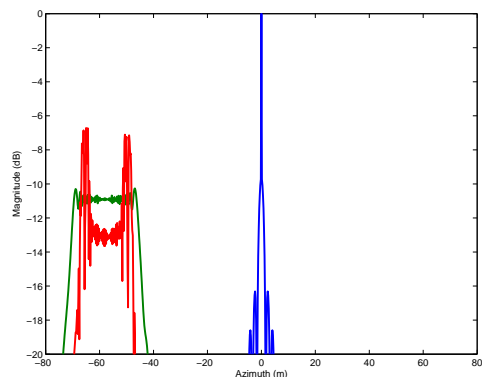


Figure 4. The effects of target motion on a standard range-Doppler processing algorithm. The blue line shows the filter response from a stationary target. The green line shows the focussing of a target with 1 ms^{-1} velocity in both the x and y directions. The red line shows the effect of adding a heave component from a 8 s (100 m) wave with amplitude of 10 cm to the moving target, when the target motion follows the sea surface.

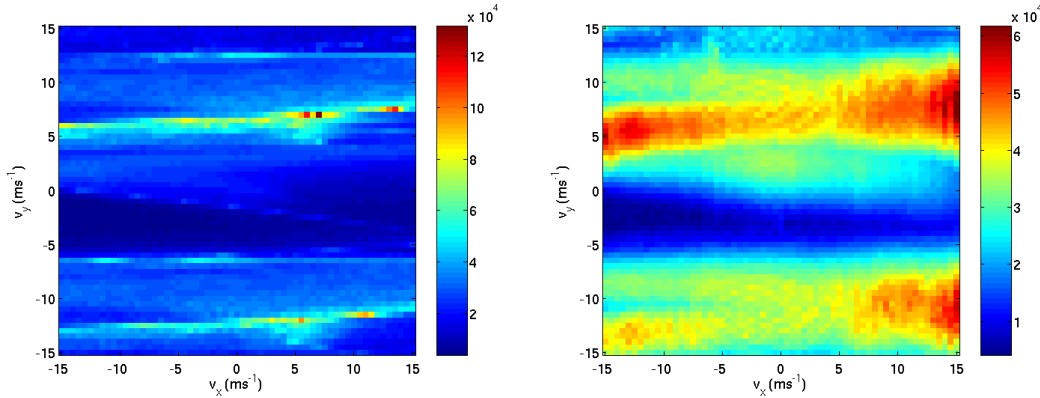


Figure 6. Two dimensional matched filter mapping for a matched filter bank with heave (left) and without vessel heave (right) included in the baseline matched filter.

To provide estimates of the velocity of the ship target, a matched filter bank may be defined based on a range of estimators \hat{v}_x and \hat{v}_y with $\hat{\zeta}(t)$ obtained from the time-frequency decomposition. The matched filter bank approach for finding the along track velocity is described, for example, in [6]. This approach uses a two dimensional matched filter bank (v_x and v_y are estimated jointly) and the nonlinear accelerations are accounted for by the “heave” function. The map, of the outputs of the matched filters for varying horizontal velocities, is thus defined as:

$$M(v_x, v_y, \hat{\zeta}) = \max |s(t) \otimes g(t, v_x, v_y, \hat{\zeta})|. \quad (5)$$

In this case, for each of v_x, v_y the reference function is convolved with the signal along a line of constant slant range. The magnitude of the response provides a measure of the focus achieved with each of the test pairs of v_x and v_y with the known $\hat{\zeta}$. The maximum response of the peak values of the matched filter mapping can then be chosen as the estimate of the along and across track velocities: \hat{v}_x and \hat{v}_y , respectively.

Figure 6 shows the application of a matched filter bank with both v_x and v_y defined on the range $[-15, 15]$ ms^{-1} with $\Delta v = .2 \text{ ms}^{-1}$. The plot on the left hand side of this figure shows the results with $\hat{\zeta}$ included. The right hand plot shows the results without considering the accelerations extracted from the time-frequency representation. The broad nature of the mapping without heave shows that accelerations present in the signal are not accounted for in the matched filter. The sharper focus of the mapping on the left indicates that the $\hat{\zeta}$ has accounted for much of the acceleration in the signal data.

4 VERIFICATION

The methodology has been confirmed by experimental data from two different field trials. Maritime trials of the ATI SAR were conducted offshore Nova Scotia in March, 2004 and more recently on the Grand Banks, offshore Newfoundland, during June, 2006.

During the 2004 experiment, two cooperating vessels from the Canadian Coast Guard were instrumented with Global Positioning System (GPS) receivers to record position and velocity. The vessels, a 16 m cutter and a 68 m patrol vessel, were in relatively calm waters (approximately 1 m significant wave height) for the duration of the imaging. Taking the GPS record as ground truth, the root mean square error (rmse) in velocity estimation is 1.0 ms^{-1} for the heave compensated estimates versus an rmse of 2.8 ms^{-1} for the matched filter bank without heave compensation.

The 2006 experiment offshore Newfoundland employed ships of opportunity and relied on the Automatic Information System (AIS) reporting of vessel position and velocity. The M/V Green Guatemala was imaged in seas recorded as growing from 2.0 to 2.6 m significant wave height during the aircraft flight on 12 June (approximately a 4 hour window close to the imaging time). Application of the model to this vessel provided estimates of along and across track velocities that were within cms^{-1} of the velocities reported by the AIS. In

this case, the AIS reported a velocity of 6.6 ms^{-1} (along track) and 6.97 ms^{-1} (across track): The algorithm estimated $\hat{v}_x = 6.76 \text{ ms}^{-1}$ and $\hat{v}_y = 6.97 \text{ ms}^{-1}$. This result is for a large vessel in low to moderate seas and may not be completely representative. The rmse estimates for velocity from the March 2004 trial may be more representative (where an rmse of 1.0 ms^{-1} between ground truth and estimated along track velocity was found). Validation efforts are on-going and a ship trial to capture the behaviour of a vessel in high sea states is planned.

Heave was estimated for the M/V Green Guatemala by an inversion of (4) with the across track acceleration assumed to be negligible. The components estimated provided heave amplitudes of 1, 0.8, 0.1, and 0.5 m with wavelengths of encounter of 83, 291, 24, and 517 m. These estimates are probable for the observed sea conditions: waves above 2 m significant with multimodal seas and winds close to 20 knots. Validation of the heave extraction will require an experiment with a vessel instrumented to record vessel motion. Confirmation of the heave signature could have implications for studying the ocean surface wave regime through an understanding of the expected vessel dynamics.

The improvement in focus resulting from the inclusion of the heave trace in the matched filter process is shown in Figure 7. The graphic shows a 3dB increase in magnitude and the response width reduced by a factor of 2 in azimuth. The inclusion of the heave function does not provide a perfectly focused target but there is a definite improvement in focus from the case where heave is ignored.

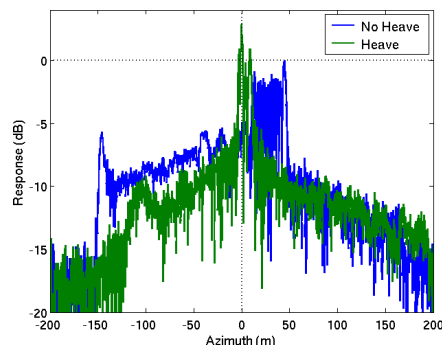


Figure 7. The improvement in focus of the M/V Green Guatemala with heave compensation. The green line shows a 3 dB improvement in target return strength and a reduction in azimuth smearing of 1/2.

Figure 8 shows the results of the azimuth compression with heave (left) and for the best filter response without considering heave (right). The inclusion of the heave estimate, $\hat{\zeta}$, in the final application of an azimuth matched filter, provides sharper focus and the correct azimuth positioning of the target response. The best filter response without heave (produced using (5) with the ζ function set to zero) occurred at 19.5 ms^{-1} and -4.9 ms^{-1} in the along and across track directions, respectively.

5 CONCLUSION

The focussing of ship targets by identifying the contribution of heave motion in the Doppler frequency signature has been described. The use of a matched filter which includes estimation of heave provides an improvement

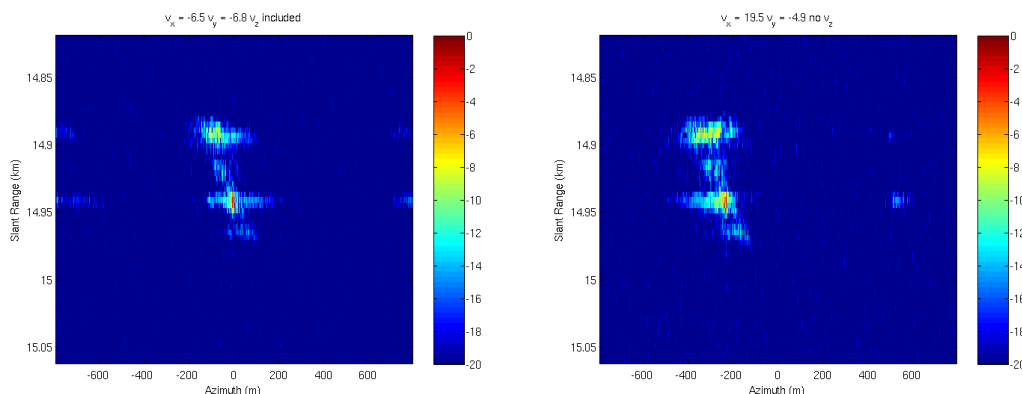


Figure 8. Azimuth compressed imagery of the M/V Green Guatemala with heave included(left) and best estimate without heave compensation (right).

in the accuracy of the estimation of along track velocity and azimuth focussing of a vessel. While a follow-on experiment would be necessary to confirm the estimation of heave, the methodology does point to a clear means of observing the dynamics of a ship at sea using a SAR. Determining efficient processing methodologies to automatically extract heave and then focus target signatures for surveillance applications is the subject of continuing research at Defence R&D Canada – Ottawa.

REFERENCES

- [1] RANEY, R. K., “Synthetic aperture imaging radar and moving targets,” *Aerospace and Electronic Systems, IEEE Transactions on* **AES-7**(3), pp. 499–505, 1971.
- [2] BARBAROSSA, S., “Detection and imaging of moving objects with synthetic aperture radar. Part 1: Optimal detection and parameter estimation theory,” *IEE Proceedings-F* **139**(1), pp. 79–88, 1992.
- [3] DRAGOŠEVIĆ, M. V. AND S. S. STANKOVIC, “An adaptive notch filter with improved tracking properties,” *Signal Processing, IEEE Transactions on* **43**, pp. 2068–2078, 1995.
- [4] RIECK, W., “SAR imaging of moving targets: Application of Time-Frequency distribution for single- and multichannel data,” in *Proceedings EUSAR’96*, pp. 431–434, VDE-Verlag GMBH, (Berlin), 1996.
- [5] SHARMA, J. J., C. H. GIERULL, AND M. J. COLLINS, “The influence of target acceleration on velocity estimation in dual-channel SAR-GMTI,” *Geoscience and Remote Sensing, IEEE Transactions on* **44**, pp. 134–147, 2006.
- [6] SHARMA, J. J., C. H. GIERULL, AND M. J. COLLINS, “Compensating the effects of target acceleration in dual-channel SAR-GMTI,” *IEEE Proceedings on Radar, Sonar, and Navigation* **153**(1), pp. 53–62, 2006.
- [7] VACHON, P. W., AND M. V. DRAGOŠEVIĆ, “COASP and CHASP processors for strip-map and moving target adaptive processing of EC CV-580 synthetic aperture radar data: Algorithms and software description,” Tech. Rep. TM 2006-066, Defence R&D Canada – Ottawa, May 2006.
- [8] LIVINGSTONE, C. E., A. L. GRAY, R. K. HAWKINS, P. W. VACHON, T. I. LUKOWSKI, AND M. LALONDE, “The CCRS airborne SAR systems: Radar for remote sensing research,” *Canadian Journal of Remote Sensing* **21**(4), pp. 468–491, 1995.
- [9] VACHON, P. W., M. V. DRAGOŠEVIĆ, N. KASHYAP, C. LIU, D. SCHLINGMEIER, A. MEEK, T. POTTER, B. YUE, AND J. KRAFT, “Processing and analysis of polarimetric ship signatures from MARSIE report on results for polar epsilon,” Tech. Rep. TM 2006-202, Defence R&D Canada – Ottawa, October 2006.
- [10] CUMMING, I. G., AND F. H. WONG, *Digital Processing of Synthetic Aperture Radar Data: Algorithms and Implementation*, Artech House, Boston, 2005.
- [11] KONG, Y.-K., B.-L. CHO, AND Y.-S. KIM, “Ambiguity-free doppler centroid estimation technique for airborne sar using the radon transform,” *Geoscience and Remote Sensing, IEEE Transactions on* **43**, pp. 715–721, April 2005.
- [12] CUMMING, I. G., AND S. LI, “Improved slope estimation for SAR doppler ambiguity resolution,” *Geoscience and Remote Sensing, IEEE Transactions on* **44**, pp. 707–718, 2006.
- [13] CHEN, V. C., AND H. LING, *Time-frequency transforms for radar imaging and signal analysis*, Artech House, Inc., Norwood, MA, 2002.
- [14] KORENBERG, M. AND K. ADENEY, “Iterative fast orthogonal search for modelling by a sum of exponentials or sinusoids,” *Annals of Biomedical Engineering* **141**, pp. 315–327, 1998.
- [15] MCGAUGHEY, D., *Spectral Modelling and Simulation of Atmospherically Distorted Wavefront Data*. Ph.D. thesis, Queen’s University, Kingston, ON, Canada, 1999.